

The impact of misregistration on SRTM and DEM image differences

Thomas G. Van Niel^{a,d,*}, Tim R. McVicar^{b,d}, LingTao Li^{b,d}, John C. Gallant^b, QinKe Yang^c

^a CSIRO Land and Water, Private Bag No. 5, Wembley, WA 6913, Australia

^b CSIRO Land and Water, GPO Box 1666, Canberra, ACT 2601, Australia

^c Institute of Soil and Water Conservation, Chinese Academy of Sciences and Ministry of Water Resources,
26 Xinong Road, Yangling, Shaanxi Province 712100, China

^d eWater Cooperative Research Centre, Building 15, University of Canberra, Canberra, ACT 2601, Australia

Received 2 May 2007; received in revised form 13 November 2007; accepted 17 November 2007

Abstract

Image differences between Shuttle Radar Topography Mission (SRTM) data and other Digital Elevation Models (DEMs) are often performed for either accuracy assessment or for estimating vegetation height across the landscape. It has been widely assumed that the effect of sub-pixel misregistration between the two models on resultant image differences is negligible, yet this has not previously been tested in detail. The aim of this study was to determine the impact that various levels of misregistration have on image differences between SRTM and DEMs. First, very accurate image co-registration was performed at two study sites between higher resolution DEMs and SRTM data, and then image differences (SRTM–DEM) were performed after various levels of misregistration were systematically introduced into the SRTM data. It was found that: (1) misregistration caused an erroneous and dominant correlation between elevation difference and aspect across the landscape; (2) the direction of the misregistration defined the direction of this erroneous and systematic elevation difference; (3) for sub-pixel misregistration the error due solely to misregistration was greater than, or equal to the true difference between the two models for substantial proportions of the landscape (*e.g.*, greater than 33% of the area for a half-pixel misregistration); and (4) the strength of the erroneous relationship with aspect was enhanced by steeper terrain. Spatial comparisons of DEMs were found to be sensitive to even sub-pixel misregistration between the two models, which resulted in a strong erroneous correlation with aspect. This misregistration induced correlation with aspect is not likely specific to SRTM data only; we expect it to be a generic relationship present in any DEM image difference analysis.

© 2007 Elsevier Inc. All rights reserved.

Keywords: Change detection; Image difference; Error; Spatial structure; Digital surface models; Murrumbidgee; Murray–Darling; Australia; Yellow River; YanHe; Loess Plateau; China; Vegetation height

1. Introduction

Misregistration has previously been shown to substantially increase the amount of change detected when using image differencing techniques on land cover images (Dai & Khorram, 1998; Townshend et al., 1992; Verbyla & Boles, 2000; Wang & Ellis, 2005). While image difference techniques are also commonly used between DEMs, the purpose is not usually to assess elevation change, but rather: (1) to assess vertical or horizontal accuracy (Guth, 2006; Hofton et al., 2006; Rodriguez et al., 2006; Simard et al., 2006; Smith & Sandwell, 2003); or for the

case of SRTM, (2) to measure features above ground-level, such as vegetation height (Carabajal & Harding, 2006; Hofton et al., 2006; Kellndorfer et al., 2004; Simard et al., 2006) or glacier volume (Berthier et al., 2006).

While some studies have quantified the misregistration between SRTM and higher resolution DEMs (Hofton et al., 2006; Rodriguez et al., 2006; Smith & Sandwell, 2003), and others have assessed the impact that misregistration has on land cover change detection (Dai & Khorram, 1998; Townshend et al., 1992; Verbyla & Boles, 2000; Wang & Ellis, 2005), to our knowledge the impact of misregistration on DEM image differences has not previously been inspected. We argue that the continuous and comparatively smooth nature of DEMs makes them influenced by misregistration differently than typical land

* Corresponding author. Tel.: +61 8 9333 6705.

E-mail address: Tom.VanNiel@csiro.au (T.G. Van Niel).

cover images, and because of this, they will usually be more affected by slight amounts of misregistration. In our literature review of studies using image-based DEM differences, we found that many authors do not report whether spatial registration between the two DEMs (co-registration) was even performed (e.g., Kellndorfer et al., 2004). Other times authors only report that the co-registration was sub-pixel, without specifying what it was (e.g., Simard et al., 2006). This indicates that misregistration between the two DEMs, or at least misregistration below 1 pixel, is very often thought to be an unimportant influence on DEM image difference. Here we test this theory by specifically assessing the sensitivity of elevation model image differences to sub-pixel misregistration between DEMs, using SRTM data as an example. Our aim is not to draw conclusions regarding the absolute vertical nor horizontal accuracy of the SRTM dataset, but rather to inspect the affect that relative spatial error in the co-registration between SRTM and DEM has on resultant image differences.

2. Background to misregistration of image differences

The underlying process driving the impact of misregistration on image differences is the same whether a DEM comparison or a land cover comparison is performed. However, as the nature of land cover surfaces is generally quite different from DEM surfaces, the associated impact misregistration has on the resultant image difference analysis is also different. The two main processes determining the impact of misregistration in any image difference are: (1) the rate of per-pixel change of the surface attribute; and (2) the level of misregistration in both x and y directions across the image (Stow, 1999; Stow & Chen, 2002). Adapted from Stow and Chen (2002), the Misregistration Noise Equivalent (MNE) is calculated as:

$$\text{MNE} = (D_{xy})(\Delta z_{xy}) \quad (1)$$

where D_{xy} represents the overall misregistration error considering both x and y directions; z is the attribute value (elevation for DEMs, but also may represent a category in a land cover classification, or Normalised Difference Vegetation Index (NDVI) value in a land cover image); Δz_{xy} is the overall rate of change, considering both x , and y directions and is calculated as:

$$\Delta z_{xy} = \left(\left(\frac{\Delta z}{\Delta x} \right)^2 + \left(\frac{\Delta z}{\Delta y} \right)^2 \right)^{0.5} \quad (2)$$

where $\frac{\Delta z}{\Delta x}$ and $\frac{\Delta z}{\Delta y}$ are the individual x and y directional rates of change.

In Stow (1999), Δz_{xy} was calculated using a central difference (i.e., the mean of ± 1 pixel from either side of the pixel of interest), which results in Δz_{xy} being equivalent to the finite difference calculation of slope (Gallant & Wilson, 2000), and thus has particular meaning to DEM users. In Stow and Chen (2002), Δz_{xy} used the pixel of interest and one neighbouring pixel in both x and y directions, depending on the local

direction of misregistration, and thus would be better described as ‘image gradient’ as this is a non-standard definition of slope in the context of DEM analysis. Importantly, Townshend et al. (1992) showed that the impact of misregistration in vegetation change detection was higher in areas of higher NDVI signal (i.e., in densely vegetated areas versus sparsely vegetated areas) because of the increased heterogeneity and associated increased Δz_{xy} when transitioning across varying vegetation types (Stow, 1999; Stow & Chen, 2002). In sparsely vegetated areas, the NDVI signal would be homogeneously low and would therefore have little to no Δz_{xy} .

Previous research addressing the issue of misregistration of image differences has solely concentrated on land cover change detection. As opposed to the relatively continuous nature of DEMs, land cover data tend to change across the landscape in a more discontinuous fashion, where attributes change abruptly when a boundary between differing cover types is reached. The extreme example of this is when land cover is classified (e.g., Verbyla & Boles, 2000; Wang & Ellis, 2005), resulting in Δz_{xy} being zero everywhere except at boundaries between classes (see Fig. 1a,b). DEM data, in contrast, are dominated by continuous change, so unlike land cover change detection, the same amount of misregistration is likely to produce lower-level differences over all of the image rather than higher-level difference only at isolated areas of abrupt change (Fig. 1b). Fig. 1b demonstrates why the emphasis of edges is often easily identified in land cover change detection, whereas the ubiquitous lower-level bias in DEM difference is not as clearly associated with misregistration. Rather, this bias can easily be misidentified as actual error structure because it has sensible spatial structure; it is related to the true landform, being a dampened and out-of-phase version of the original DEM-like profile (compare Fig. 1a,b). Furthermore, as even low levels of misregistration (i.e., sub-pixel) will likely affect the bulk of the area over a smooth DEM-like image difference surface, it is particularly important to inspect the sensitivity of the special case of DEM differencing at the sub-pixel level.

For a smooth DEM-like surface, there are two important characteristics to note regarding slope (Fig. 1c) and aspect (Fig. 1d). First, because slope is always positive, it tends to have a positive relationship with image difference over roughly half of the area and a negative relationship with the other half, resulting in a negligible overall correlation between image difference and slope (see the position of the (+) and (–) symbols in Fig. 1a and compare black lines between Fig. 1b,c). Secondly, although the association between the difference profile and aspect is not nearly perfect, a general agreement will be seen over a typical elevation profile (i.e., the black lines in Fig. 1b,d roughly rise and fall together), resulting in a strong overall correlation between image difference and aspect. This is mostly because the points of largest change in the aspect profile (Fig. 1d) match the ridges and valleys of the original profile (Fig. 1a,d). Put another way, the ridges and valleys are where the difference between the two smooth DEMs is zero (i.e., the places where the original and misregistered profiles intersect, see Fig. 1b). This means that entire hillslopes will be positively biased until a ridge or valley is reached, and then the opposing hillslope will be negatively

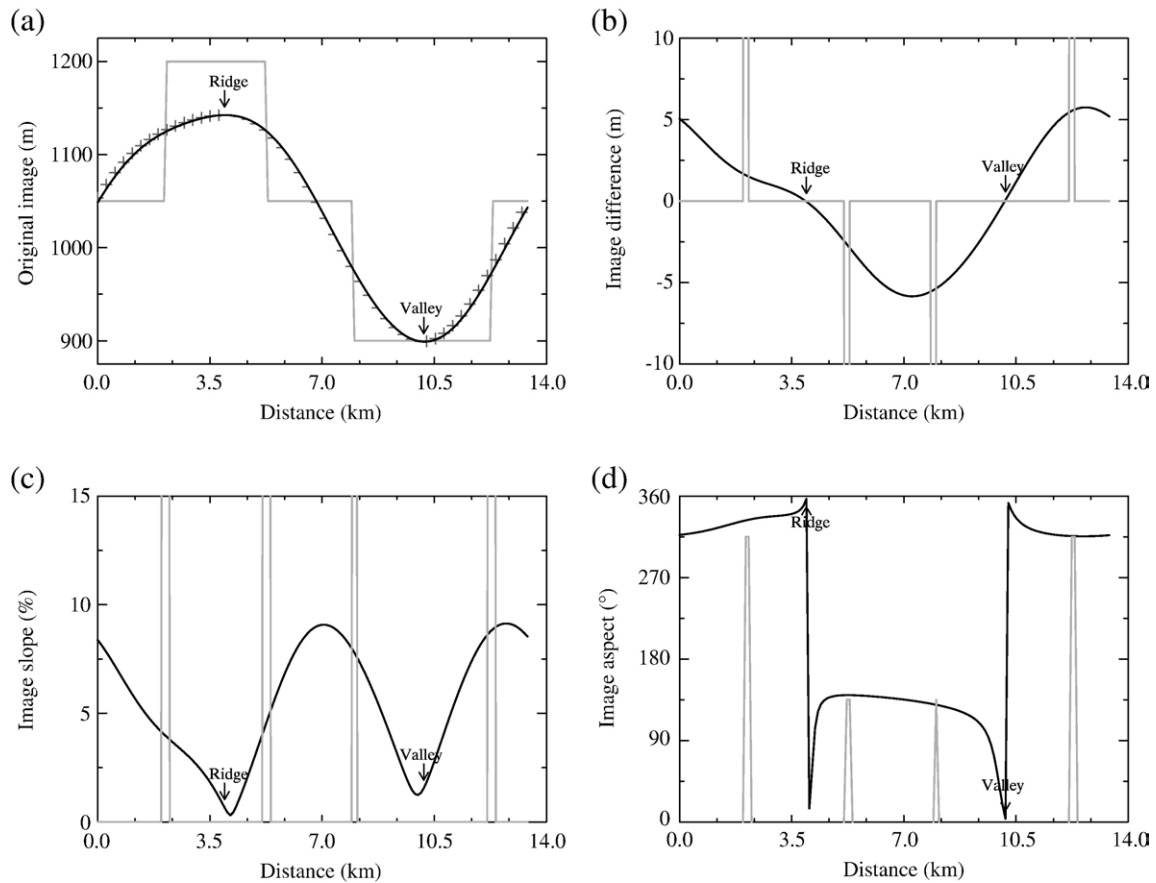


Fig. 1. The effect of misregistration between 2 continuous profiles and between 2 discontinuous profiles is illustrated. In (a), a hypothetical smooth surface (black line) illustrative of a DEM-like surface was classified (grey line) in order to represent a land cover profile that changes abruptly between class boundaries. In (b), the original profiles were shifted by 1 pixel (90 m) to the west (left) and the original profiles were subtracted from their associated shifted profiles. The slope and aspect of the original profiles are given in (c) and (d) respectively. Note, the (+) and (-) symbols in (a) represent where the shifted continuous surface is higher or lower than the original profile, respectively; the grey lines extend to ± 150 m in (b) and $\pm 118\%$ in (c); and the 'Ridge' and 'Valley' labels refer to the location of the maximum and minimum positions for the original continuous profile in (a).

biased (see the position of (+) and (-) symbols in Fig. 1a). The implication of this is that the entire landscape could be artificially correlated to aspect due to only a slight misregistration between the two DEMs being compared. Conversely, for image differences of classified images, the slope and aspect continue to act as edge detectors (see the grey lines in Fig. 1c,d). It is worth noting that if the absolute value of image difference is inspected, then the strong overall correlation seen for the DEM-like surface will be associated with slope and the negligible correlation will be with aspect.

Both Townshend et al. (1992) and Dai and Khorram (1998) conclude that to acquire a $\leq 10\%$ error in detected land cover change due to misregistration, accuracy of the registration needs to be ≤ 0.2 of a pixel. However, both of these studies achieved this recommendation by interpolation of results, as little (Townshend et al., 1992) and none (Dai & Khorram, 1998) of the misregistration was actually measured at the sub-pixel level. As shown above, this recommendation should not be generically applied as the impact of misregistration will depend on Δz_{xy} (Stow, 1999; Stow & Chen, 2002; Townshend et al., 1992), and thus will impact steeper areas (*i.e.*, Δz_{xy} is high) more than flatter areas. To our knowledge, the current

study is the first assessment of the impact of misregistration on image differences between DEMs, and also the first to measure the importance of sub-pixel level misregistration between DEMs.

3. Study sites

Two study sites were used in this investigation: (1) the Middle and Upper Murrumbidgee Catchments (MUMC), in south eastern Australia; and (2) the YanHe Basin (YHB), in north central China (Fig. 2). The MUMC is 33,696 km², centred around 35.2° S and 148.4° E. It has a moderately steep terrain, with a mean slope of 11.6% (standard deviation = 13.1%) and an elevation range between 160 m and 2045 m (mean = 680 m; standard deviation = 351 m) defined from a 25 m resolution DEM described below. The MUMC receives an average of 812 mm a⁻¹ of precipitation (standard deviation = 161 mm a⁻¹) based on spatially interpolated meteorological data from 1980 through 2000 (Jeffrey et al., 2001) and vegetation cover is mainly evergreen *Eucalyptus* forests up to 45 m canopy height, interspersed with some dryland winter cereal cropping and grasslands used for pasture. The YHB is 7701 km², centred

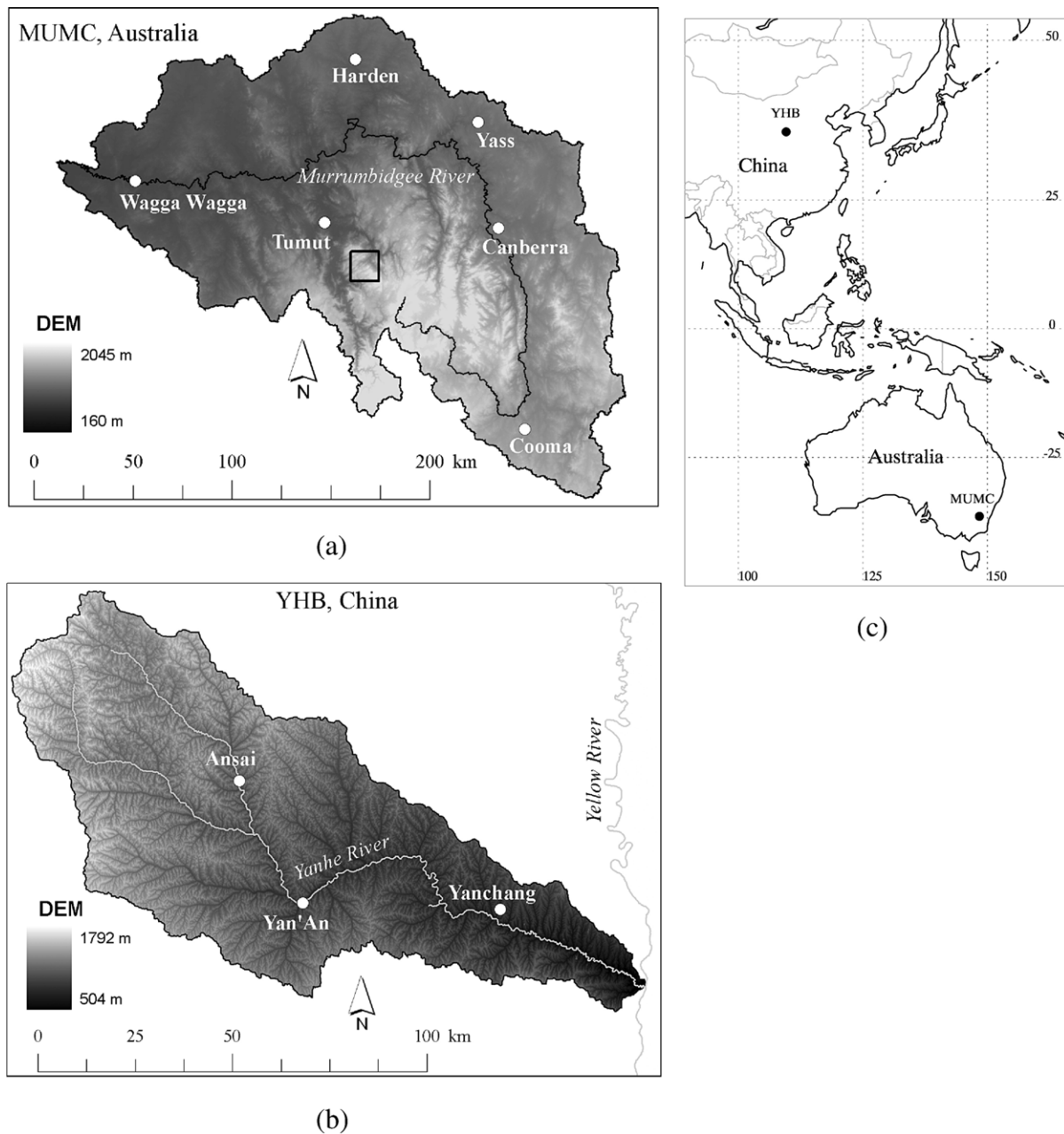


Fig. 2. Study site locations and the fine resolution DEMs are shown for (a) the MUMC; and (b) the YHB. The regional placement of the study sites is shown in (c). The box in (a) defines the area surrounding a transect demonstrated in Fig. 7.

around 36.7°N and 109.6°E . It has very steep terrain (see Fig. 3 of Yang et al., 2005) and a high gully density (Fu et al., 2006). The YHB has a mean slope of 31.5% (standard deviation=15.7%) and an elevation range between 504 m and 1792 m (mean=1214 m; standard deviation=187 m) defined from a 25 m resolution DEM described below. The average precipitation in the YHB is 475 mm a^{-1} (standard deviation=89 mm a^{-1}) based on spatially interpolated meteorological data from 1980 through 2000 (McVicar et al., 2007). The vegetation cover of the YHB is predominantly shrub-steppe with very little to no tree canopy (see McVicar et al., 2005) with some mixed

conifer and deciduous forests up to 10 m canopy height in the southern portion of the study site.

4. Data

The SRTM C-band Interferometric Synthetic Aperture Radar (InSAR) sensor (5.6 cm, 5.3 GHz) was attached to the Space Shuttle Endeavor during its mission between 11 and 22 February 2000, when it measured the Earth's surface elevation between 60°N and 56°S latitudes (Hensley et al., 2000). SRTM version 2 “finished” data were downloaded from the NASA ftp

site (<ftp://e0srp01u.ecs.nasa.gov/srtm/version2/SRTM3/>) over the MUMC and YHB in 1° by 1° tiles, which were merged and then subset to the study site extents. SRTM version 2 data are available at 90 m spatial resolution with pre-processing including correction for spikes, wells and water bodies. The 30 m SRTM data were aggregated to 90 m pixels by NASA using averaging methods. The SRTM data used in this research were not affected by the half-pixel shift as was the USGS seamless data prior to February 2007.

Existing higher resolution DEMs at the study sites were used as reference data. The 25 m spatial resolution YHB DEM was generated from drainage data, spot heights and 40 m contour interval data using ANUDEM (Hutchinson, 2004) following the methods of Yang et al. (2007) with special attention given to reducing input data source errors and defining optimal interpolation parameters. The 25 m spatial resolution MUMC DEM was generated by ANUDEM from the New South Wales Digital Topographic Data Base 10 and 20 m interval contours, spot heights and drainage data, and was expected to meet the Australian mapping standards where the majority of the dataset should have a vertical accuracy within 1/2 of contour interval and a horizontal accuracy of within 0.5 mm of the map scale (approximately 5–10 m). As the objective of this research was to assess the impact of misregistration on resultant image difference calculations, and not to quantify the misregistration of the SRTM data, it was not necessary to perform detailed positional and vertical accuracy assessments of these existing higher resolution DEMs. Specifically, we do not assume that the registration of the DEMs is “truth” as the misregistration could be primarily due to either the SRTM or the higher resolution DEM as was the case for Smith and Sandwell (2003); in reality, there will be misregistration in both datasets.

One of the major potential sources of error in SRTM data is vegetation (Carabajal & Harding, 2006; Hofton et al., 2006; Kellndorfer et al., 2004; Simard et al., 2006). In order to summarise the vegetation component at both study sites, MODIS data were obtained. As the shuttle mission was flown in February of 2000, it was mid-summer in Australia and mid-winter in China. For the MUMC, green vegetation will be primarily associated with perennial evergreen vegetation (trees) at that time of year as grasses will have senesced (Lu et al., 2003), and winter cereal crops will have been harvested. Therefore, a February NDVI image should be closely related to the presence of trees in the MUMC. The bi-weekly 250 m NDVI composite for 02 to 17 February 2001 was used (as the first MODIS NDVI imagery was only available from April 2000, hence the SRTM and MODIS could not temporally intersect, and conditions in consecutive Februaries were similar) in the MUMC. Due to data availability and little to no NDVI signal in winter in the YHB (due to dormant summer pastures and little evergreen tree cover), the MODIS Vegetation Continuous Fields (VCF) Yearly L3 500 m percent tree cover composite for 2001 (Hansen et al., 2002) was used in the YHB. This dataset estimates the percent tree cover by making use of imagery throughout the year and should provide the best estimate of SRTM error due to vegetation for the YHB.

5. Methods

The effect of misregistration error on the difference between DEMs was summarised in order to: (1) characterise this relationship specifically for elevation models while concentrating on sub-pixel level misregistration; (2) determine how much of the landscape was considerably impacted by misregistration error (*e.g.*, where elevation difference due to misregistration \geq actual elevation difference); (3) assess how misregistration impacted explanatory variables describing the spatial error structure; and (4) provide an example of how misregistration might impact an application of vegetation analysis. For topic (4) we assess a transect across a vegetated portion of the MUMC in a region where tree height can exceed 40 m.

First, the two 25 m DEMs were resampled to 90 m spatial resolution in order to match the SRTM dataset. This was done by area weighted averaging, as was done by NASA in the resampling of the 30 m SRTM data to 90 m. Next, 15 ground control points (GCPs) were collected at each study site in order to assess the accuracy of the initial registration between corresponding SRTM and DEM datasets. After initial registration accuracy was assessed, very accurate co-registration was implemented using a modification of the methods presented in Hofton et al. (2006), and Rodriguez et al. (2006). SRTM data were systematically shifted in both *x* and *y* directions to a precision of 1/25th of a grid-cell (or 3.6 m) increment. After each shift, the image difference was calculated and the Moran's I autocorrelation index was measured on the image difference using the Queen's case with a lag of 1 (Hofton et al., 2006 used standard deviation as opposed to Moran's I). The best registration was determined by the shift that produced the minimum spatial autocorrelation, and was then used for each site as the basis for the subsequent misregistration sensitivity analysis. This methodology was preferred to standard image registration as very high accuracy (*e.g.*, within <0.1 pixel) is difficult to obtain when gathering GCPs between two elevation models. The method used here works best when the first order misregistration error between datasets is represented by a single offset.

Table 1
Description of datasets used in the current study

Variable	Description
SRTM ϵ -orig	Misregistered SRTM data as originally downloaded.
SRTM ₀	Best-case registration SRTM data.
SRTM ϵ	Misregistered SRTM data after misregistration error was systematically introduced to SRTM ₀ . ϵ is the misregistration error in units of fraction of 90 m pixel (0.125, 0.25, 0.5, or 1.0).
SRTM ₀ -DEM	Elevation difference between SRTM ₀ and the DEM; this variable is also called “actual” elevation difference because it includes minimal influence by misregistration.
SRTM ϵ -DEM	Elevation difference between misregistered SRTM data and the DEM.
SRTM ϵ -SRTM ₀	Absolute value of the elevation difference due solely to misregistration.
SRTM ϵ -SRTM ₀ / SRTM ₀ -DEM	Absolute value of the elevation difference due solely to misregistration relative to the absolute value of the actual elevation difference; referred to as “relative difference” in Table 3.

The best-case registered SRTM dataset is denoted $SRTM_0$; a list of variable names and a brief description of all datasets used in this study is provided in Table 1.

To quantify the sensitivity of image differences to misregistration, spatial misregistration errors (ϵ) were introduced systematically to the best-case registration in all 8 neighbouring directions by a factor of 0.125, 0.25, 0.5, and 1.0 of the pixel size (*i.e.*, 11.25 m, 22.5 m, 45 m, and 90 m in this case). Sub-pixel misregistration was achieved by oversampling $SRTM_0$ to a finer resolution based on the specified fraction of the original pixel size (*e.g.*, 0.5 of the original pixel size, or 45 m), shifting the finer resolution dataset by one oversampled pixel (*e.g.*, 0.5 of the original pixel size, or 45 m), then aggregating the shifted version back to the original 90 m pixel size using area weighted averaging. The best-case registered and the perturbed SRTM datasets were compared to the DEM to define image differences representing the actual elevation difference ($SRTM_0 - DEM$) and the error affected elevation difference ($SRTM_\epsilon - DEM$), see Table 1. The error due to misregistration alone was also determined by the absolute value of the $SRTM_\epsilon$ dataset minus the best-case SRTM dataset ($|SRTM_\epsilon - SRTM_0|$).

The relationship between image difference and aspect was used to summarise error structure. The aspect surface determined from the high resolution DEM for each study site was

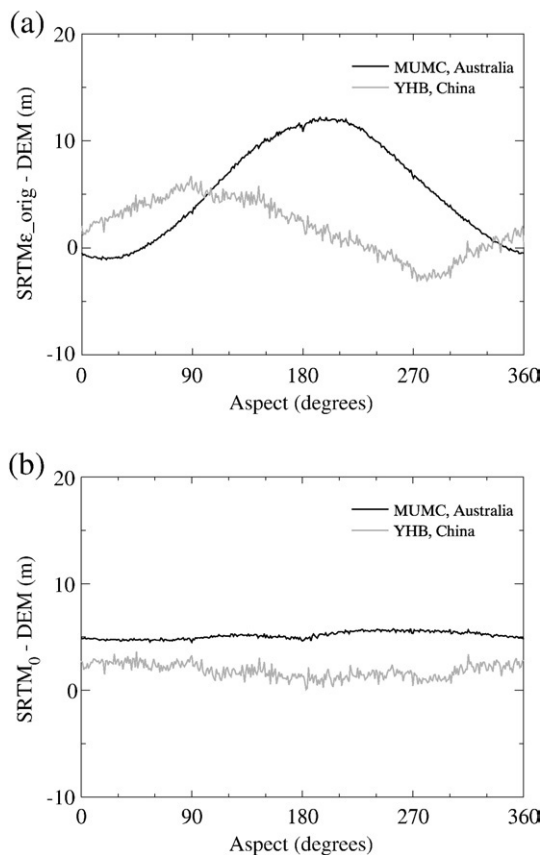


Fig. 3. The relationship between aspect and elevation model difference is shown (a) for the initial co-registration (RMSD was 0.53 pixel for MUMC and 0.25 pixel for YHB); and (b) after very accurate co-registration (RMSD <0.04 pixel for both MUMC and YHB).

classified into 360 classes, one per each degree of aspect. For each aspect class, the mean of each $SRTM_\epsilon - DEM$ image was determined and plotted, thus characterising the relationship.

The sensitivity of image differences were also summarised using the complement of the cumulative distribution function, which is generally termed the ‘empirical quantile function’ or the ‘flow duration curve’ when measuring stream flow in hydrologic applications (Vogel & Fennessey, 1994). When used in hydrology, the flow duration curve estimates the percentage of time a particular stream flow was equalled or exceeded (Vogel & Fennessey, 1994). For our purposes, the empirical quantile function measured the percentage of total study site area where a particular elevation difference was equalled or exceeded. The elevation difference metric in this case was the amount of elevation difference due to misregistration alone relative to the actual elevation difference when no misregistration was present. First, the absolute value of the mean difference in elevation of the 4 cardinal neighbours due to misregistration alone ($|SRTM_\epsilon - SRTM_0|$) was calculated at each misregistration level over the entire study site, resulting in 4 spatial datasets per study site. Then, each of these were divided by the absolute value of the actual elevation difference (*i.e.*, $|SRTM_0 - DEM|$), resulting in another 4 spatial datasets per study site. These final datasets provided a metric of how large the elevation differences caused by misregistration errors were relative to the actual elevation differences between models. The percentage of the total area for the range in $|SRTM_\epsilon - SRTM_0|/|SRTM_0 - DEM|$ values were assessed. This allowed the area with an elevation difference due solely to misregistration that equalled or exceeded the actual elevation difference to be calculated.

Different mechanisms of error can be expected to be correlated with landscape metrics in different ways; smoothing for example, raises locally low elevations and reduces locally high elevations. We explored the impact of misregistration error on the correlation coefficient of determination (r^2) for 4 landscape variables: (1) aspect; (2) slope; (3) topographic position index (TPI); and vegetation characteristics from either MODIS NDVI (for the MUMC) or MODIS VCF (for the YHB). TPI is expressed in metres and is calculated by determining the relative topographic position of the centre cell to the average of its neighbours in a 5 by 5 window (*e.g.*, Lapen & Martz, 1996); negative TPI values indicate that a point is lower than the surrounding topography, positive TPI values indicate that it is higher than the surrounding topography, and values of (or near) zero indicate that a point in the landscape is at the same (or similar) elevation to the surrounding landscape or that it is near the mid-slope of a hill. The r^2 was calculated between: (1) $SRTM_\epsilon - DEM$ difference images in each of the 8 neighbouring directions for each of the 4 levels of misregistration error (0.125, 0.25, 0.5, and 1.0 of the 90 m pixel size); and (2) each of the 4 landscape variables mentioned above, calculated from the high resolution DEM for each study site. Results of this analysis show whether (and by how much) misregistration error caused the variables explaining the variance in the image difference to change.

Finally, a demonstration of the potential impact misregistration error can have on vegetation analysis is provided. Misregistration

Table 2
Range of elevation differences (m) for the aspect relationship for the 4 levels of misregistration is shown

Direction	SRTM ϵ –DEM (m)							
	MUMC				YHB			
	ϵ 0.125	ϵ 0.25	ϵ 0.50	ϵ 1.00	ϵ 0.125	ϵ 0.25	ϵ 0.50	ϵ 1.00
West	3.5	5.8	10.2	19.3	6.2	11.0	20.8	41.1
North	3.0	5.1	9.7	19.0	7.4	11.5	20.4	38.1
East	2.1	4.4	8.9	18.2	7.7	12.6	22.3	42.0
South	3.1	5.2	9.7	19.0	5.6	9.4	18.0	35.9
SRTM ₀ –DEM	1.3	1.3	1.3	1.3	3.6	3.6	3.6	3.6

The columns labelled ϵ 0.50 in this table are associated with Fig. 4. For example, the range in elevation differences for a 0.50 pixel shift to the West at the YHB resulted in a maximum difference of 12.4 m near 270°, and a minimum difference of -8.4 m near 90° for an elevation range of 20.8 m (see the grey line in Fig. 4a).

could cause significant errors in estimation of vegetation heights calculated from the difference between SRTM and a bare-earth DEM, particularly in steep areas. A single 150 pixel transect across a tall forested area in the MUMC was analysed over SRTM ϵ –DEM image differences (ϵ =0.5 pixel in the four cardinal directions) and were compared to the transect for the best-case registration (SRTM₀–DEM) image difference. For these 5 image differences, the slope of the trend line was determined, and whether the slope was significantly different

from zero was assessed at the 95% confidence interval. The r^2 was calculated between each of the 4 SRTM ϵ –DEM image differences and the SRTM₀–DEM best-case registration image difference. The Root-Mean-Squared Difference (RMSD) and index of agreement (d) were also calculated (Willmott et al., 1985) comparing each systematically perturbed transect with the best-case transect:

$$RMSD = \left[\frac{1}{n} \sum_{i=1}^n (P_i - O_i)^2 \right]^{0.5} \tag{3}$$

$$d = 1 \left[\frac{\sum_{i=1}^n (P_i - O_i)^2}{\sum_{i=1}^n (|P_i - \langle O \rangle| + |O_i - \langle O \rangle|)^2} \right] \tag{4}$$

where n =number of observations (150); P =the predicted variable; with O and $\langle O \rangle$ =the observed variable, and the mean of the observed variable, respectively. For this assessment, P =SRTM ϵ –DEM and O =SRTM₀–DEM.

6. Results and discussion

The initial registration of the SRTM data downloaded from the NASA ftp site for the MUMC had an RMSD of 0.53 pixels

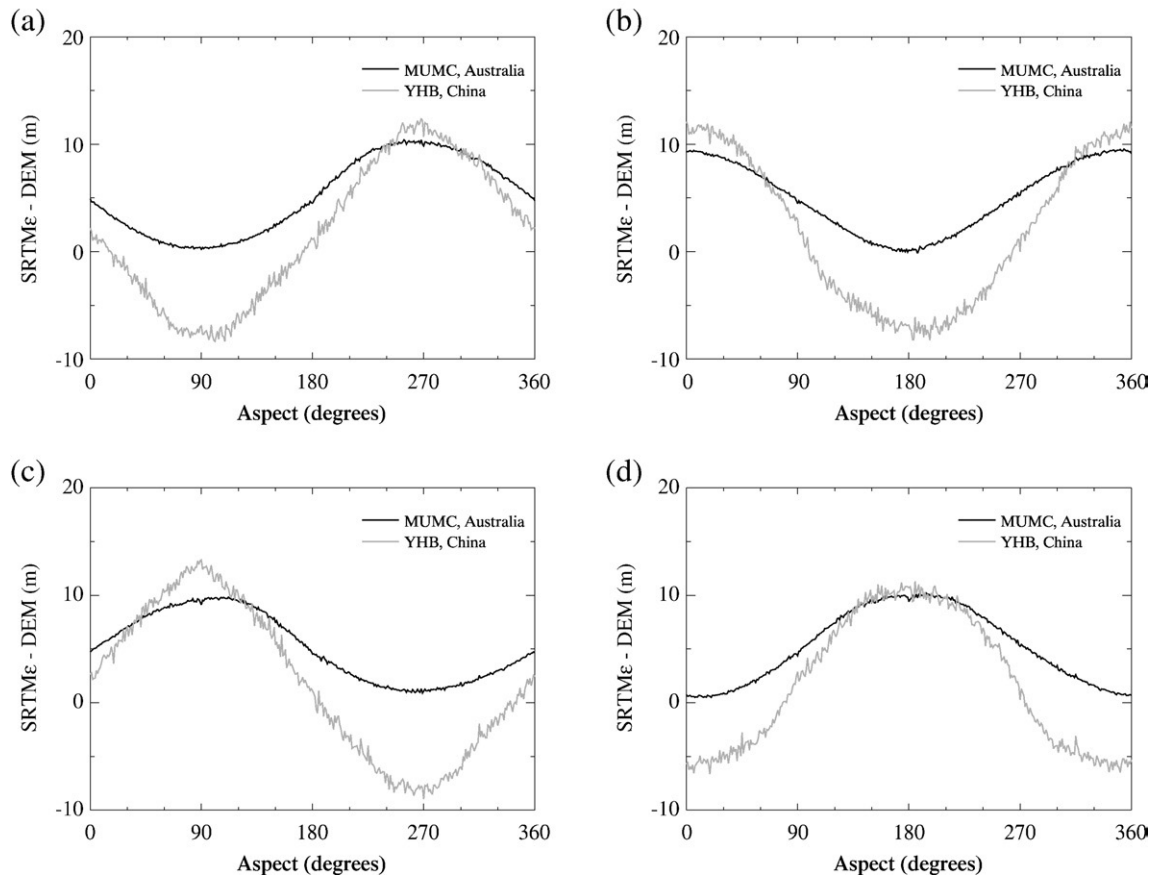


Fig. 4. The relationship between aspect and elevation model difference is shown after a 0.5 pixel misregistration was introduced (ϵ =0.5) in the four cardinal directions of (a) west; (b) north; (c) east; and (d) south.

or 47.7 m, and the YHB had an RMSD of 0.25 pixels or 22.5 m. These initial registrations resulted in the systematic offsets associated with aspect in the $SRTM_0$ –DEM elevation differences shown in Fig. 3a as noted by Jarvis et al. (2004). Each was sine-like in shape with a different phase and order of magnitude. It is noteworthy that although the initial co-registrations at both study sites were well under a pixel, they both demonstrated strong relationships between elevation difference and aspect (Fig. 3a). This is particularly important as sub-pixel misregistration is very often thought to be of negligible impact.

Co-registration between the DEMs and SRTM data at both sites was performed to a precision of 0.04 pixel, or ≤ 3.6 m. As can be seen in Fig. 3b, the systematic bias is mostly removed after accurate co-registration was applied, indicating that the strong relationship between image difference and aspect (Fig. 3a) was largely due to misregistration. As the elevation difference was shown to be an almost constant function of aspect in Fig. 3b, this indicates an overall and evenly distributed overestimation of the elevation from SRTM when compared to the DEMs. The MUMC overestimation was higher than that observed from the YHB, consistent with the presence of tall trees in parts of the MUMC. We attribute this difference to the fact that SRTM data are not a traditional DEM, but rather a Digital Surface Model (DSM). That is, DSMs are not models of the ground elevation, but are affected by objects above the ground, such as buildings and vegetation. However, as SRTM can penetrate some distance into vegetation (depending on the vegetation density, Hofton et al., 2006; Kellndorfer et al., 2004), the difference between SRTM and ground elevation is sometimes negligible, especially for steep terrain, and short vegetation canopies (Carabajal & Harding, 2006; Hofton et al., 2006; Simard et al., 2006) such as within the YHB.

This same relationship was explored when known amounts and directions of misregistration error were systematically introduced into the best-case registration of Fig. 3b. The overall results are summarised in Table 2 for all 4 levels of misregistration (0.125, 0.25, 0.5, and 1.0 of the pixel size) for both study sites, and depicted in Fig. 4a–d for a misregistration level of 0.5 pixel ($\epsilon=0.5$) in the four cardinal directions of west, north, east, and south. As seen in Fig. 4, the overall maxima in image difference was always predominantly in the direction that the misregistration was introduced, and the overall minima was about 180° offset from this. The relationship between the curves for the MUMC and the YHB also indicated that the same amount of misregistration error resulted in an approximate doubling of elevation differences for the YHB compared to the results for the MUMC, demonstrating that the relationship was strengthened over steeper terrain (Fig. 4 and Table 2). Importantly, Table 2 and Fig. 4 show that the relationship between image differences was predictable and reproducible, further confirming that the principal cause of this relationship was indeed misregistration between the two models.

Surfaces were created over each study site that represented the relative proportion of image difference due solely to misregistration compared to actual elevation differences associated with no misregistration (*i.e.*, $|SRTM_\epsilon - SRTM_0|/|SRTM_0 - DEM|$). These were performed for each of the 4 levels of misregistration

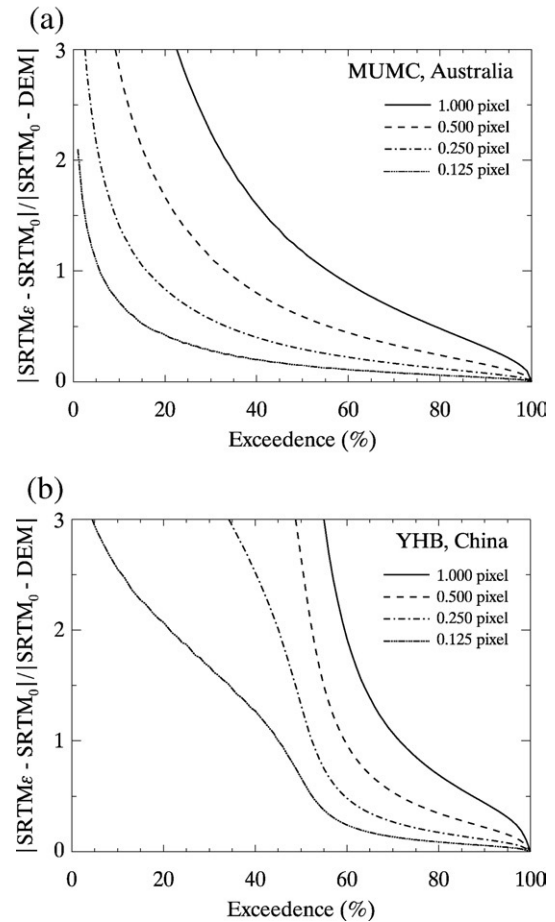


Fig. 5. The empirical quantile function of the difference due to misregistration in SRTM relative to the actual difference between the SRTM and the DEM is shown. Summaries were calculated using all 90 m pixels for both study sites (4,128,012 for the MUMC and 950,730 for the YHB).

previously introduced into the best-case registration surface ($\epsilon=0.125, 0.25, 0.5$, or 1.0), and are summarised in Fig. 5. Values on the y-axis ≥ 1 indicate where the difference due to misregistration was \geq the actual difference between models. For example, the impact of 0.5 pixel misregistration on image difference was greater than, or equal to, the actual image difference for 33% of the landscape in the MUMC, and 59% of the landscape in the YHB (Fig. 5a,b and Table 3). Fig. 5 and Table 3 show that even low levels of misregistration error caused considerable differences for large portions of the landscape at both study sites. Also, this analysis shows that misregistration alone caused the majority of both study sites to be in error by $\geq 10\%$ of the actual error for all ϵ values tested. Both Dai and Khorram (1998) and Townshend et al. (1992) recommend that a registration of 0.2 of a pixel is needed to limit the change detection error induced by misregistration to 10%. We show that even at an ϵ of 0.125, 63% and 76% of the MUMC and YHB areas, respectively equalled or exceeded the 10% elevation difference error threshold (Fig. 5 and Table 3). This difference is probably due to the dissimilar response expected from differencing two continuous and rather smooth surfaces as discussed in Section 2, above. Since sub-pixel misregistration causes as much, or more, difference than the actual difference for large portions of

Table 3
Percent study site area having differing relative amounts of image difference due solely to misregistration is summarised for the various amounts of systematically introduced misregistration at both study sites

Relative difference ^a	Area (%)							
	MUMC				YHB			
	$\epsilon 0.125$	$\epsilon 0.25$	$\epsilon 0.50$	$\epsilon 1.00$	$\epsilon 0.125$	$\epsilon 0.25$	$\epsilon 0.50$	$\epsilon 1.00$
0.1	63	84	95	99	76	91	97	100
0.5	16	34	55	79	52	59	71	87
1.0	5	16	33	55	45	52	59	71
1.5	2	9	22	42	34	48	54	63
2.0	1	6	16	33	21	45	52	59

^a Relative difference = $|SRTM\epsilon - SRTM_0| / |SRTM_0 - DEM|$ and represents the elevation difference due solely to misregistration relative to the actual elevation difference.

the landscape, both assessments of elevation models for error assessment (e.g., Guth, 2006; Hofton et al., 2006; Kenward et al., 2000), and for vegetation analysis (e.g., Kellndorfer et al., 2004) could be severely impacted if the co-registration is not very accurate.

Fig. 6 shows the correlation of SRTM error with the four landscape variables as a function of misregistration. The key results of the correlation assessment at both sites were: (1) changes in misregistration error amounts caused the amount of image difference variance explained by the variables tested to change; and (2) that a strong relationship with aspect at both sites only existed when misregistration was present. A correlation between elevation error and aspect therefore appears to be a strong indicator of misregistration. As expected of SRTM data over a vegetated site, the variance in the MUMC image difference was dominated by NDVI, but only when there was no or little misregistration (Fig. 6a). As misregistration error became >0.7 of a pixel, aspect became the dominant explanatory variable (Fig. 6a). In other words, as misregistration error increased, NDVI and slope explained less of the image difference variance, while aspect explained more; there was little trend in TPI (Fig. 6a). It is important to point out that although aspect explains a great deal of the variance of the image difference at higher levels of misregistration, this is only due to the false structure caused by misregistration. The true correlation of these variables is depicted only when there is no introduced misregistration (i.e., $SRTM_0 - DEM$); where the x -axis is equal to zero in Fig. 6. The difference between two DEMs tends to be largest where the gradient is highest, and smallest where the gradient is lowest (see Fig. 1a–b). This generally means that misregistration causes higher differences at the mid-slope where gradient is high and will be zero at the peaks and valleys of profiles where the DEM profiles intersect (see Fig. 1b). At both peaks and valleys aspect changes rapidly from, for example, north to south or from east to west; both resulting in a very discontinuous change of 180° or half of the dynamic range. This causes a strong association between a DEM image difference and aspect (Fig. 1d), and explains the fairly strong correlation seen here. It is important to note that this artificial bias has previously been incorrectly attributed to SRTM acquisition incidence angle (Jarvis et al., 2004).

Over the very steep terrain of the YHB, the dominant explanatory variable was TPI (Fig. 6b). This was probably because the high variability in local relative relief increased the instances of overestimating valley bottoms and underestimating hill tops (normal characteristics of radar-derived elevation models), thus strengthening the relationship with TPI. Hillslopes in the YHB site are much shorter than in the MUMC so the relatively coarse SRTM resolution leads to a significant reduction in local relief. Notably, the same aspect relationship was seen for the YHB as observed in the MUMC; the variance in image difference explained by aspect was near zero when there was minimal misregistration, and became increasingly strong as more misregistration was introduced (Fig. 6b). As the YHB is essentially “bald-Earth” conditions, there was no relationship between image difference variance and MODIS VCF (tree cover). There was also no relationship with slope at either site. This was because slope is not directional and is always positive so that for about half of the area, the slope would generally have a positive relationship with the image difference and for the other half it would have a negative relationship. The average effect is a weak or absent correlation with slope when considering the whole of the study area (Fig. 1c).

Several studies use image differences between SRTM and a higher resolution DEM to estimate vegetation height (e.g., Hofton et al., 2006; Kellndorfer et al., 2004; Simard et al., 2006); the

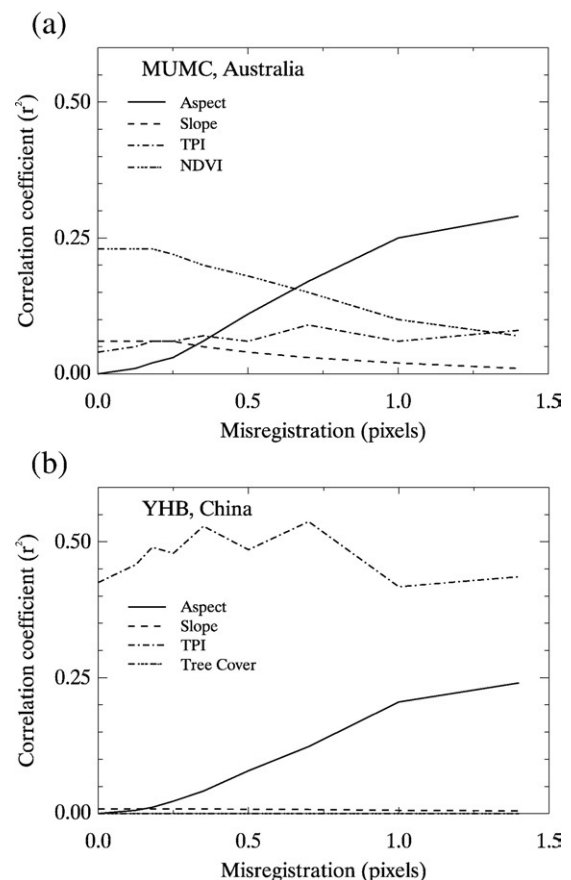


Fig. 6. The impact of misregistration on the correlation of selected dependent variables to difference between SRTM and the DEM is shown. Note, the tree cover line in (b) plots at zero for all misregistrations.

results drawn from these analyses rely heavily on empirical assessment of transects across the imagery and/or regressions with validation points. In order to provide an example of how misregistration can spatially impact vegetation height analyses, a 150-pixel transect was arbitrarily chosen from a forested portion

of the MUMC (Fig. 7). The aim of this analysis was to demonstrate whether the elevation difference due solely to misregistration could cause substantial discrepancy between the various difference images for the same transect. RMSD, d , and r^2 were calculated comparing the image differences with misregistration

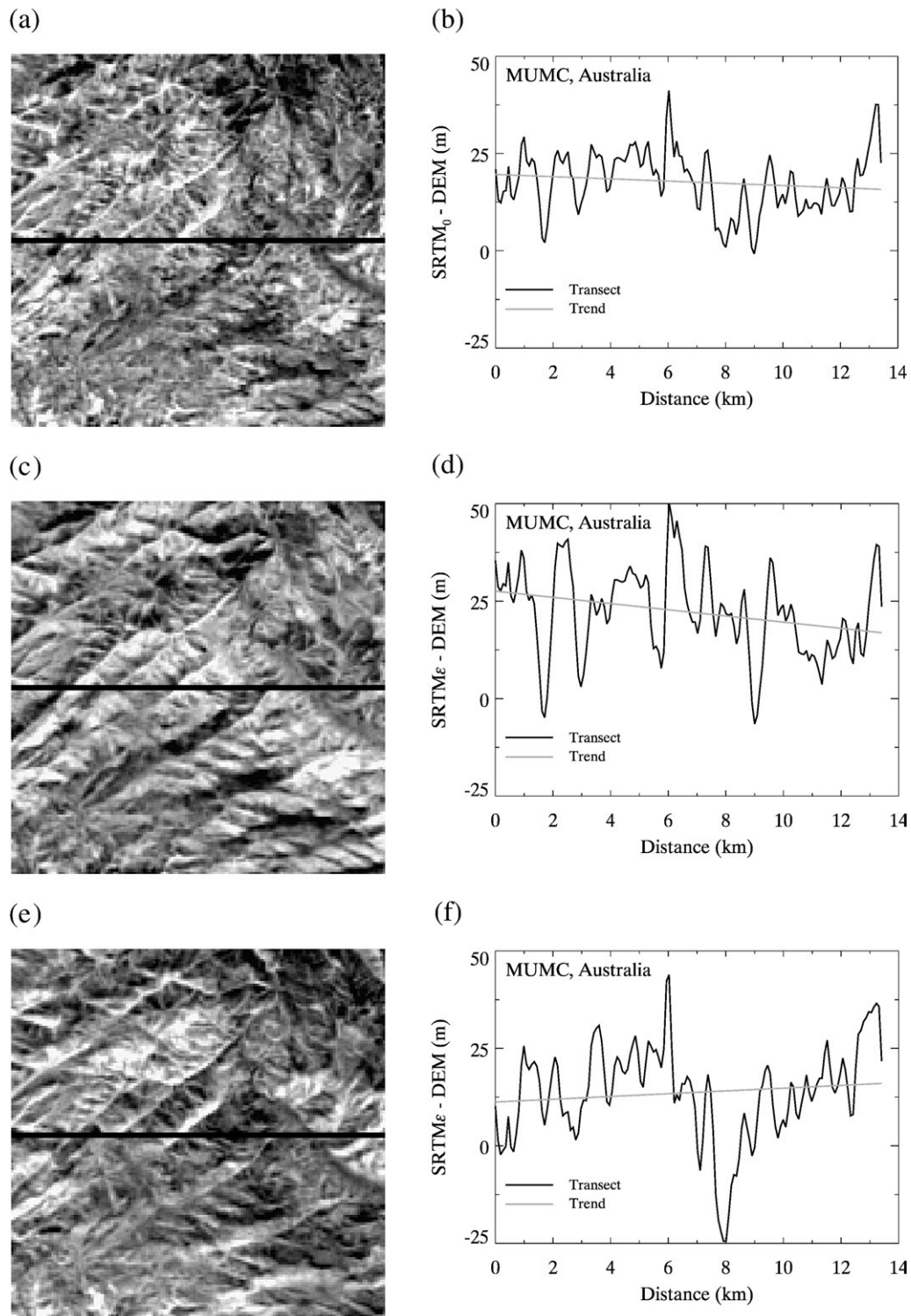


Fig. 7. 150 by 150 pixel subset of the image differences and the profile of the same transect across each; see Fig. 2 where the location is provided. The image difference and transect for the best-case registration are shown in (a) and (b); after a 0.5 pixel misregistration was introduced ($\epsilon=0.5$) to the north in (c) and (d); and after a 0.5 pixel misregistration was introduced to the south in (e) and (f). The difference images are scaled linearly between -37 m (black) and 73 m (white).

Table 4
Summary statistics of transect analysis are shown for a misregistration of 0.5 of a pixel in each of the cardinal directions

	West	North	East	South	SRTM ₀ –DEM
RMSD (m)	8.17	8.67	8.09	9.09	–
<i>d</i>	0.69	0.68	0.70	0.65	–
<i>r</i> ²	0.73	0.58	0.31	0.59	–
Trend slope (m km ⁻¹)	-0.18	-0.79 ^a	-0.32	0.35	-0.29

^a Significantly different from a slope of zero at the 95% confidence level.

error in the 4 cardinal directions (SRTM_ε–DEM) to the best-case registration image difference (SRTM₀–DEM), see Table 4. The RMSD and *d* metrics were in relative agreement, where the RMSD was higher in the north and south-shifted image differences, which resulted in lower *d* values. These two misregistration directions are highlighted in Fig. 7. Introducing a 0.5 pixel shift resulted in the strong erroneous association with aspect, which is clearly seen in both the disparity between the best-case image difference (Fig. 7a) and its associated transect (Fig. 7b) and the misregistered image differences and transects (Fig. 7c–f). Of particular interest was how the trend of the best-case registered image difference was decreasing along the transect, but not significantly so (Table 4, and Fig. 7a,b). However, a misregistration of 0.5 pixel to the north changed the transect values enough to make the trend of the transect significant at the 95% confidence level (Table 4). Furthermore, a 0.5 pixel shift to the south, caused enough difference to switch the sign of

the trend’s slope to positive (Fig. 7f and Table 4), demonstrating how sensitive image difference values along a transect can be to misregistration. We also note that the elevation differences for the best-case registered image are all positive (Fig. 7b), consistent with the hypothesis that the elevation errors are due to trees increasing the measured heights. In the misregistered cases there are some negative differences that are not consistent with errors induced by trees (Fig. 7d,f).

Further study could examine whether the 30 m SRTM data are as highly sensitive to sub-pixel shifts. The distance term *D*_{xy} in the MNE (Eq. (1)) is measured in metres, not pixels, so larger pixels with the same amount of *D*_{xy} would cause higher MNE for sub-pixel misregistrations than smaller pixels—if *D*_{xy} was the only consideration. However, over the same terrain, larger pixels have reduced slopes (Hutchinson and Gallant, 2000), therefore Δ*z*_{xy} (Eq. (1)) will be higher for smaller pixels than for larger pixels. This compensatory effect would make the MNE lower for larger pixels—if Δ*z*_{xy} was the only consideration. Whether sub-pixel misregistration impacts larger or smaller pixels differently at a given site depends on the relative amounts of *D*_{xy} and Δ*z*_{xy} to the pixel sizes being considered. These considerations may also be influenced, in the case of SRTM, by its effective resolution (Guth, 2006; Smith & Sandwell, 2003); noting that misregistration amount (*D*_{xy} in metres not proportions of pixels) is the same for the 30 m and 90 m SRTM data.

Fig. 8 shows the scatter plots of the image differences having a 0.5 pixel misregistration in all 4 cardinal directions when

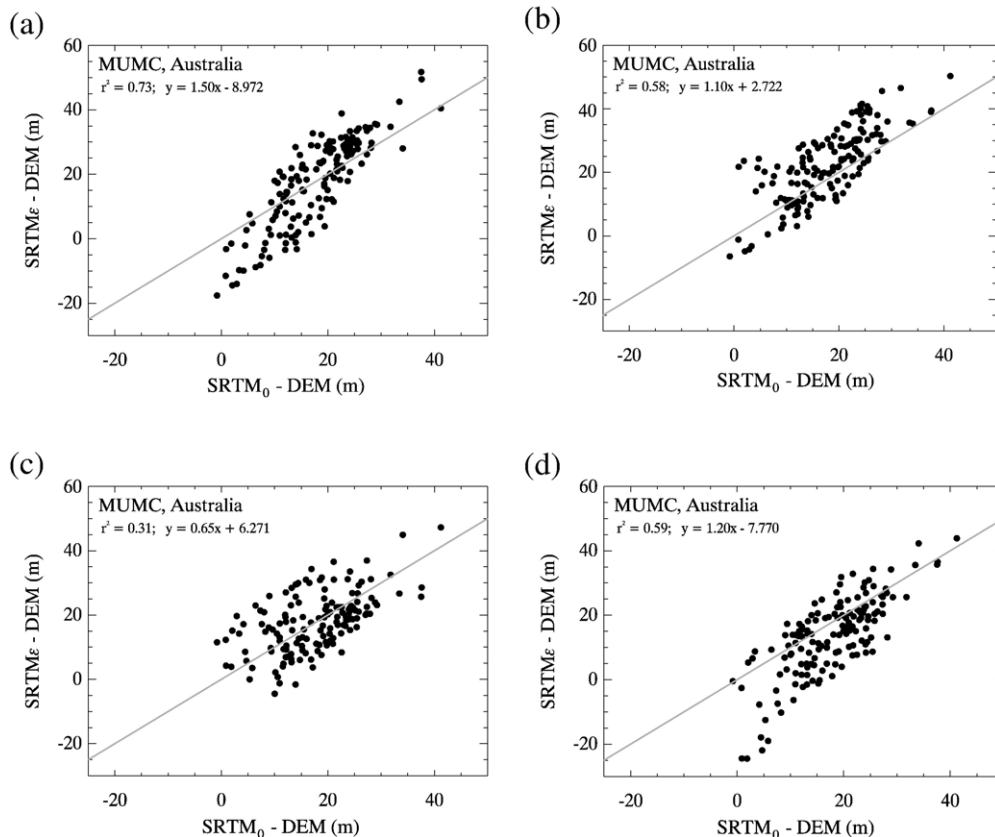


Fig. 8. Scatter plots of image difference values across the 150 pixel transect are shown between the best-case registration (x-axes) compared to the various image differences after a misregistration of 0.5 pixel ($\epsilon=0.5$) was introduced to the (a) west; (b) north; (c) east; and (d) south. The 1:1 line is drawn in grey.

compared to the best-case registration for the transects previously presented. Fig. 8 and Table 4 show that the r^2 , and the offset and slope of the linear regression between the various image differences was quite variable, ranging between 0.31 and 0.73, -8.97 m to 6.27 m, and 0.65 to 1.50 , respectively. This also quantified the impact that misregistration alone can have on image difference-type analyses. This example clearly demonstrated that misregistration can substantially change the elevation difference values along a transect, and that these changes can significantly change the slope of the trend line ($P=0.05$ see Table 4). As elevation profiles are often used to draw conclusions and develop scientific theories (e.g., Kellndorfer et al., 2004), this analysis shows the importance of accurate co-registration. Importantly, it validated the results shown in Fig. 5 that misregistration caused substantial discrepancies in image differences that were a similar order of magnitude of the actual elevation differences. It also showed that very detailed examination of transects across image differences is probably unadvisable for study sites having moderately steep or greater slopes (similar to the study sites here) unless misregistration is almost eliminated because both the magnitude and slope of the image difference transect as well as the r^2 can change substantially due to sub-pixel misregistration.

It is apparent from the different offsets used to register the SRTM to the DEM at the MUMC and YHB that misregistration is not a simple global offset. The length scale over which the misregistration varies has not been explored. Further study could examine the smallest area of DEM required to reliably measure misregistration by the appearance of aspect-correlated errors and the length scale over which the misregistration of SRTM data varies. Many applications of the SRTM data would benefit from a map of misregistration error or a corrected DEM that removed the misregistration. This might be performed at a continental level in order to identify errors associated with continental processing differences if they exist. However, whenever a different DEM is compared to SRTM, it would result in a different co-registration relationship as the misregistration can be due to either the SRTM or the DEM, or both. As shown here, it is critical to remove the misregistration-induced bias between elevation models before performing image differences.

7. Conclusions

Very few studies regarding image differences of DEMs report, or likely even assess, the level of misregistration between DEMs. We expect that most researchers believe that co-registration errors <1 pixel are insignificant, yet we showed that misregistration ≤ 0.5 pixel substantially impacted estimation of elevation difference between SRTM and DEMs at two study sites. The main conclusions of this research include:

- (1) Misregistration caused an erroneous and strong correlation between aspect and elevation difference. When very little misregistration existed between SRTM and DEM, there was very little correlation between elevation

difference and aspect. With increasing misregistration, the true dominant correlates became weaker until they were replaced by aspect. For example, at the Australian site we found that aspect became a stronger correlate with spatial error structure than slope when $\varepsilon \geq 0.35$ (± 0.04) of a pixel shift was introduced and stronger than NDVI when $\varepsilon \geq 0.70$ (± 0.04) of a pixel shift was introduced.

- (2) The relationship between aspect and error structure was expressed as a sinusoidal wave with its phase determined by the direction of the misregistration between the two elevation models.
- (3) At both study sites, the error due solely to misregistration was greater than or equal to the true difference between SRTM and DEM for substantial proportions of the landscape, even for small levels of misregistration. For example, the difference due to shifting SRTM by a quarter of a pixel was greater than or equal to the true difference between SRTM and DEM for 16% of the area at the Australian site and 52% of the area at the Chinese site. Both Dai and Khorram (1998) and Townshend et al. (1992) concluded that registration within 0.2 of a pixel was needed to limit the change detection difference induced by misregistration to 10%, yet between SRTM and DEM we show that even at 0.125 of a pixel, the majority of both the Australian and Chinese study sites (63% and 76%, respectively) equalled or exceeded 10% elevation difference due to misregistration.
- (4) Overall, the strength of the relationship between error structure and aspect was enhanced in steeper terrain, verifying the fundamental assumptions of Stow (1999) and Stow and Chen (2002). This demonstrated the importance of minimising misregistration between elevation models, particularly over steeper terrain where a small misregistration between the two models can dominate the differences in elevation.

These results show that image differences between DEMs are sensitive to even small amounts of misregistration between the two DEMs. DEM image differences are more sensitive to sub-pixel misregistration than standard land cover change detection because of the smooth and continuous nature of DEM data. The sensitivity to sub-pixel misregistration will depend on the effective resolution of the datasets being compared (Guth, 2006; Smith & Sandwell, 2003) and the relative importance of the D_{xy} and Δz_{xy} terms of the MNE (Eq. (1)) at a given site for various pixel sizes. It has been shown that misregistration is the source of the strong correlation between SRTM and DEM elevation difference and aspect. Not understanding this relationship could easily lead to misunderstanding the source and nature of the differences between DEMs.

Acknowledgements

Thanks to Dr Greg Summernell, NSW Department of Natural Resources, for providing access to the 25 m resolution DEM for the MUMC as part of the eWater CRC Project D1, Linda Gregory,

CSIRO Land and Water, for downloading and mosaicking of the SRTM data for the MUMC, Dr Mike Roderick, the Australian National University, for the IDL code for testing the significance of the slope of the trend line, and Dr Doug Ramsey for providing DEMs over Utah, USA, which were not used in the paper, but helped us to assess the aspect relationship reported. Part of this work was funded by ACIAR LWR/2002/018, eWater CRC project D1, CSIRO Land and Water, and CSIRO Water for a Healthy Country Flagship. Thanks to Dan Pollock and Geoff Hodgson, CSIRO Land and Water, and two anonymous reviewers and the editor for their helpful comments that improved the paper.

References

- Berthier, E., Arnaud, Y., Vincent, C., & Remy, F. (2006). Biases of SRTM in high-mountain areas: Implications for the monitoring of glacier volume changes. *Geophysical Research Letters*, *33*, L08502.
- Carabajal, C. C., & Harding, D. J. (2006). SRTM C-band and ICESat laser altimetry elevation comparisons as a function of tree cover and relief. *Photogrammetric Engineering and Remote Sensing*, *72*, 287–298.
- Dai, X., & Khorram, S. (1998). The effects of image misregistration on the accuracy of remotely sensed change detection. *IEEE Transactions on Geoscience and Remote Sensing*, *36*, 1566–1577.
- Fu, B. J., Zhang, Q. J., Chen, L. D., Zhao, W. W., Gulincik, H., Liu, G. B., Yang, Q. K., & Zhu, Y. G. (2006). Temporal change in land use and its relationship to slope degree and soil type in a small catchment on the Loess Plateau of China. *Catena*, *65*, 41–48.
- Gallant, J. C., & Wilson, J. P. (2000). Primary topographic attributes. In J. P. Wilson, & J. C. Gallant (Eds.), *Terrain Analysis* (pp. 51–85). New York: John Wiley & Sons, Inc.
- Guth, P. L. (2006). Geomorphometry from SRTM: Comparison to NED. *Photogrammetric Engineering and Remote Sensing*, *72*, 269–277.
- Hansen, M., DeFries, R., Townshend, J., Sohlberg, R., Dimiceli, C., & Carroll, M. (2002). Towards an operational MODIS continuous field of percent tree cover algorithm: Examples using AVHRR and MODIS data. *Remote Sensing of Environment*, *83*, 303–319.
- Hensley, S., Rosen, P., & Gurrola, E. (2000, December). Topographic map generation for the Shuttle Radar Topography Mission C-band SCANSAR interferometry. In Thomas T. Wilheit, Harunobu Masuko, & Hiroyuki Wakabayashi (Eds.), *Proceedings of SPIE — Volume 4152. Microwave Remote Sensing of the Atmosphere and Environment II* (pp. 179–189). doi:10.1117/12.410596
- Hofton, M. A., Dubayah, R., Blair, J. B., & Rabine, D. (2006). Validation of SRTM Elevations over vegetated and non-vegetated terrain using medium footprint Lidar. *Photogrammetric Engineering and Remote Sensing*, *72*, 279–285.
- Hutchinson, M. F. (2004). *ANUDEM Version 5.1 User Guide*. Canberra: The Australian National University, Centre for Resource and Environmental Studies. <http://cres.anu.edu.au/outputs/software.php>
- Hutchinson, M. F., & Gallant, J. C. (2000). Digital elevation models and representation of terrain shape. In J. P. Wilson, & J. C. Gallant (Eds.), *Terrain Analysis* (pp. 29–50). New York: John Wiley & Sons, Inc.
- Jarvis, A., Rubiano, J., Nelson, A., Farrow, A., & Mulligan, M. (2004). 'Practical use of SRTM data in the tropics — Comparisons with digital elevation models generated from cartographic data.' Centro Internacional de Agreicultura Tropical (CIAT). <http://srtm.csi.cgiar.org/PDF/Jarvis4.pdf>
- Jeffrey, S. J., Carter, J. O., Moodie, K. B., & Beswick, A. R. (2001). Using spatial interpolation to construct a comprehensive archive of Australian climate data. *Environmental Modelling and Software*, *16*, 309–330.
- Kellndorfer, J., Walker, W., Pierce, L., Dobson, C., Fites, J. A., Hunsaker, C., Vona, J., & Clutter, M. (2004). Vegetation height estimation from Shuttle Radar Topography Mission and National Elevation Datasets. *Remote Sensing of Environment*, *93*, 339–358.
- Kenward, T., Lettenmaier, D. P., Wood, E. F., & Fielding, E. (2000). Effects of Digital Elevation Model accuracy on hydrologic predictions. *Remote Sensing of Environment*, *74*, 432–444.
- Lapen, D., & Martz, L. (1996). An investigation of the spatial association between snow depth and topography in a Prairie agricultural landscape using digital terrain analysis. *Journal of Hydrology*, *184*, 277–298.
- Lu, H., Raupach, M. R., McVicar, T. R., & Barrett, D. J. (2003). Decomposition of vegetation cover into woody and herbaceous components using AVHRR NDVI time series. *Remote Sensing of Environment*, *86*, 1–18.
- McVicar, T. R., Li, L. T., Van Niel, T. G., Hutchinson, M. F., Mu, X. M., & Liu, Z. H. (2005). 'Spatially Distributing 21 Years of Monthly Hydrometeorological Data in China: Spatio-Temporal Analysis of FAO-56 Crop Reference Evapotranspiration and Pan Evaporation in the Context of Climate Change.' CSIRO Land and Water Technical Report, 8/05, Canberra, Australia. <http://www.clw.csiro.au/publications/technical2005/tr8-05.pdf>
- McVicar, T. R., Van Niel, T. G., Li, L. T., Hutchinson, M. F., Mu, X. M., & Liu, Z. H. (2007). Spatially distributing monthly reference evapotranspiration and pan evaporation considering topographic influences. *Journal of Hydrology*, *338*, 196–220.
- Rodriguez, E., Morris, C. S., & Belz, J. E. (2006). A global assessment of the SRTM performance. *Photogrammetric Engineering and Remote Sensing*, *72*, 249–260.
- Simard, M., Zhang, K., Rivera-Monroy, V. H., Ross, M. S., Ruiz, P. L., Castaneda-Moya, E., Twilley, R. R., & Rodriguez, E. (2006). Mapping height and biomass of mangrove forests in Everglades National Park with SRTM elevation data. *Photogrammetric Engineering and Remote Sensing*, *72*, 299–311.
- Smith, B., & Sandwell, D. (2003). Accuracy and resolution of shuttle radar topography. *Geophysical Research Letters*, *30*, 1467.
- Stow, D. A. (1999). Reducing the effects of misregistration on pixel-level change detection. *International Journal of Remote Sensing*, *20*, 2477–2483.
- Stow, D. A., & Chen, D. M. (2002). Sensitivity of multitemporal NOAA AVHRR data of an urbanizing region to land-use/land-cover changes and misregistration. *Remote Sensing of Environment*, *80*, 297–307.
- Townshend, J. R. G., Justice, C. O., Gurney, C., & McManus, J. (1992). The impact of misregistration on change detection. *IEEE Transactions on Geoscience and Remote Sensing*, *30*, 1054–1060.
- Verbyla, D. L., & Boles, S. H. (2000). Bias in land cover change estimates due to misregistration. *International Journal of Remote Sensing*, *21*, 3553–3560.
- Vogel, R. M., & Fennessey, N. M. (1994). Flow-duration curves I: New interpretation and confidence intervals. *Journal of Water Resources Planning and Management*, *120*, 485–504.
- Wang, H., & Ellis, E. C. (2005). Image misregistration error in change measurements. *Photogrammetric Engineering & Remote Sensing*, *71*, 1037–1044.
- Willmott, C. J., Ackleson, S. G., Davis, R. E., Feddema, J. J., Klink, K. M., Legates, D. R., O'Donnell, J., & Rowe, C. M. (1985). Statistics for the evaluation and comparison of models. *Journal of Geophysical Research*, *90*, 8995–9005.
- Yang, Q. K., McVicar, T. R., Van Niel, T. G., Hutchinson, M. F., Li, L. T., & Zhang, X. P. (2007). Improving a digital elevation model by reducing source data errors and optimising interpolation algorithm parameters: An example in the Loess Plateau, China. *International Journal of Applied Earth Observation and Geoinformation*, *9*, 235–246.
- Yang, Q. K., Van Niel, T. G., McVicar, T. R., Hutchinson, M. F., & Li, L. T. (2005). Developing a digital elevation model using ANUDEM for the Coarse Sandy Hilly Catchments of the Loess Plateau, China.' CSIRO Land and Water Technical Report 7/05, Canberra, Australia. <http://www.clw.csiro.au/publications/technical2005/tr7-05>